2D simulation of chemotactic bacteria aggregation

Americo Marrocco

INRIA

INSTITUT NATIONAL DE RECHERCHE EN INFORMATIQUE ET EN AUTOMATIQUE

2D simulation of chemotactic bacteria aggregation

A. Marrocco

N° 4667

Décembre 2002

THÈME 4

ISSN 0249-6399

INRIA
ROCQUENCOURT

2D simulation of chemotactic bacteria aggregation

A. Marrocco*

Thème 4 — Simulation et optimisation
de systèmes complexes
Projet M3N

Rapport de recherche n° 4667 — Décembre 2002 — 26 pages

Abstract: We start from a mathematical model which describes the collective motion of bacteria taking into account the underlying biochemistry. This model was first introduced by Keller-Segel [1]. A new formulation of the system of partial differential equations is obtained by the introduction of a new variable (this new variable is similar to the quasi-Fermi level in the framework of semiconductor modelling). This new system of P.D.E. is approximated via a mixed finite element technique. The solution algorithm is then described and finally we give some preliminary numerical results.Especially our method is well adapted to compute the concentration of bacteria.

Key-words: biophysics, chemotaxis, numerical simulation, mixed finite element

* Inria, Domaine de Voluceau, Rocquencourt BP 105 78153 Le Chesnay, France

Unité de recherche INRIA Rocquencourt
Domaine de Voluceau, Rocquencourt, BP 105, 78153 Le Chesnay Cedex (France)
Téléphone : +33 1 39 63 55 11 — Télécopie : +33 1 39 63 53 30

Simulation bidimensionnelle de l'aggrégation des bactéries

Résumé : Nous partons d'un modèle mathématique qui décrit le déplacement collectif de bactéries et qui prend en compte la biochimie sous-jacente. Ce modèle a été introduit initialement par Keller-Segel [1]. Une nouvelle formulation du système d'équations aux dérivées partielles est obtenue par l'introduction d'une variable similaire au quasi-niveau de Fermi de la modélisation des semi-conducteurs. Le nouveau système est approché par une technique d'éléments finis mixtes. On décrit ensuite l'algorithme de résolution et donnons quelques résultats numériques préliminaires. La méthode présentée est particulièrement adaptée au calcul de concentrations de bactéries

Mots-clés : biophysique, chemotaxis, simulation numérique, éléments finis mixtes

1 Problem Formulation

The equations for the collective motion of the bacteria can be derived (with no free parameters) from the underlying biochemistry. The basic equations for the bacterial density ρ and the attractant concentration c are (see [1][2][3][4])

$$\frac{\partial \rho}{\partial t} = D_b \nabla^2 \rho - \nabla \cdot (k\rho \nabla c) + a\rho \tag{1}$$

$$\frac{\partial c}{\partial t} = D_c \nabla_c^2 + \alpha\rho \tag{2}$$

where

D_b is the bacterial diffusion constant

k is the chemotactic coefficient (or chemotactic sensitivity)

a is the rate of bacterial division

α is the rate of attractant production

D_c is the chemical diffusion constant.

The terms in equation (1) include the diffusion of bacteria, chemotactic drift and division of bacteria. Equation (2) expresses the diffusion and production of attractant.

In [2] for example, typical numerical values are given for the various parameters,

$$\begin{aligned} D_b &= 7.10^{-6} \ \mathrm{cm}^2/\mathrm{s}, & D_c &= 10^{-5} \ \mathrm{cm}^2/\mathrm{s}, \\ k &= 10^{-16} \ \mathrm{cm}^5/\mathrm{s}, & \alpha &= 10^3 \ /\mathrm{s/bacteria}. \end{aligned}$$

Taking a bacterial density $\rho = 10^6/\mathrm{cm}^3$ the length scale is about 260 microns and the time scale $100s$.

In some semi-solid media (like agar), the diffusion of bacteria is much slower than attactant diffusion which motivate to drop the term with time derivative in equation (2). This limit case is also convenient for asymptotic behaviour when considering other media. Notice that for other applications, the diffusion of attractants is neglected, this is the case for angiogenesis, see [5] and the references therein.

In addition, cells divide much more slowly than the dynamics take place (the time scale for cell division is about 2 hours) so that we can take $a = 0$ in (1) for an entry level model. The model used for the numerical simulations is then the following

$$\frac{\partial \rho}{\partial t} = D_b \nabla^2 \rho - \nabla \cdot (k\rho \nabla c) \tag{3}$$

$$0 = D_c \nabla_c^2 + \alpha\rho \tag{4}$$

which we re-write (for convenience)

$$-\,\mathrm{div}(\mathrm{D_c}\,\mathrm{grad}\,\mathrm{c}) - \alpha\rho = 0 \tag{5}$$

$$\frac{\partial \rho}{\partial t} - \,\mathrm{div}(\mathrm{D_b}\,\mathrm{grad}\,\rho - \mathrm{k}\rho\,\mathrm{grad}\,\mathrm{c}) = 0. \tag{6}$$

This last formulation ((5)-(6)), strongly looks like a classical model of transient drift-diffusion of electrons in semiconductor media (nevertheless the term wich corresponds here to the attractant production is with an opposite sign). The attractant concentration c corresponds to the electrostatic potential (φ), the bacterial density ρ to the electron density (n), the chemotactic coefficient k to the electron mobility (μ_n). As in semiconductor modelling framework, a new formulation of system ((5)-(6)) will be obtained by introduction of a variable which is similar to the electron quasi-Fermi level and denoted by φ_n.

Note that we can find in the paper [2], one other formulation of eq. (4)

$$0 = D_c \nabla_c^2 + \alpha\rho\, e^{-\rho/\rho^*} \tag{7}$$

which can be used when modelling the following fact: when the bacterial density becomes too high, the bacteria consume all the food sources (succinate and oxygen) in their local environment and cease producing the attractant aspartate. The parameter ρ^* is the cutoff bacterial density.

One of the problem that has attracted biologists and mathematicians is to understand pattern formation in such models. The most noticeable, and complex also is the aggregation of bacteria [6][7][8] [2][4]. In this paper we investigate this pattern based on a mixed finite element method. We begin with another formulation based on quasi-Fermi levels, then we describe the finite element algorithm and we present in a fourth section some numerical results.

2 New Formulation of the "Chemotaxis Model"

First of all we can introduce a scaling on the c variable (attractant concentration) via the parameter q.

$$C = \frac{\widetilde{C}}{q} \tag{8}$$

The system (5)-(6), becomes

$$-\,\mathrm{div}(\mathrm{D_c}\,\mathrm{grad}\,\tilde{\mathrm{c}}) - \mathrm{q}\alpha\rho = 0 \tag{9}$$

$$\frac{\partial\rho}{\partial t} - \mathrm{div}\left[\mathrm{D_b}\,\mathrm{grad}\,\rho - \frac{\mathrm{k}}{\mathrm{q}}\,\rho\,\mathrm{grad}\,\tilde{\mathrm{c}}\right] = 0 \tag{10}$$

($+\frac{\partial\tilde{c}}{\partial t}$ could be added to the left hand side of (9) if the transient equation for the attractant diffusion was considered). We introduce a new variable φ_n by setting

$$\rho = \rho(\tilde{c}, \varphi_n) = \rho_0\, e^{\frac{\tilde{c}+\varphi_n}{Z}} \tag{11}$$

where

- ρ_0 is a constant (which corresponds to a given bacterial density, the variable $\tilde{c}$ and φ_n (or their sum) are then equal to zero)
- $z = \dfrac{q\,D_b}{k}$.

This class of variables is useful because we expect high values of ρ (collapse) and the potential φ_n is a more reasonable quantity. The system of equations can now be written as

$$-\,\mathrm{div}(\mathrm{D_c}\,\mathrm{grad}\,\tilde{\mathrm{c}}) - \tilde{\alpha}\rho(\tilde{\mathrm{c}}, \varphi_{\mathrm{n}}) = 0 \tag{12}$$

$$\frac{\partial \rho(\tilde{c},\varphi_n)}{\partial t} - \operatorname{div}(\tilde{\mathrm{k}}\rho(\tilde{\mathrm{c}},\varphi_{\mathrm{n}})\operatorname{grad}\varphi_{\mathrm{n}}) = 0 \tag{13}$$

where

$$\tilde{k} = k/q, \quad \tilde{\alpha} = \alpha q$$

The system of equation (12)-(13) where the unknowns are $\tilde{c}$ and φ_n will be used for the numerical approximation. This system has to be completed with appropriate boundary condition on $\tilde{c}$ and φ_n and initial condition for the bacterial density ρ.

Eq. (12) is similar to the Poisson equation and eq. (13) to the electron continuity equation in the semiconductor framework.

3 Mixed Finite Element Approximation and Solution Algorithm

3.1 Numerical approximation (M.F.E.)

Following [9][10][11][12], and assuming that Dirichlet boundary condition on a part of the boundary (Γ_d) – of the computational domain Ω – and Neumann boundary condition on the complementary boundary part (Γ_n) hold for the variables $\tilde{c}$ and φ_n, we introduce the flux variables

$$\vec{V} = D_c \operatorname{grad}\tilde{\mathrm{c}} \quad , \quad \tilde{\mathrm{J}}_\rho = \tilde{\mathrm{k}}\rho(\tilde{\mathrm{c}},\varphi_{\mathrm{n}})\operatorname{grad}\varphi_{\mathrm{n}} \quad , \tag{14}$$

and an equivalent formulation of the system (12)-(13)

$$\begin{cases} -\operatorname{div}\tilde{\mathrm{V}} - \tilde{\alpha}\rho(\tilde{\mathrm{c}},\varphi_{\mathrm{n}}) = 0 & \text{in } \Omega \quad (15) \\ \vec{V} = D_c \operatorname{grad}\tilde{\mathrm{c}} & \text{in } \Omega \quad (16) \\ \vec{V}\cdot\vec{n} = D_c \cdot f_{1n} & \text{on } \Gamma_{n1} \quad (17) \\ \tilde{c} = f_{1d} & \text{on } \Gamma_{d1} \quad (18) \end{cases}$$

$$\begin{cases} \dfrac{\partial \rho(\tilde{c},\varphi_n)}{\partial t} - \operatorname{div}\tilde{\mathrm{J}}_\rho = 0 & \text{in } \Omega \quad (19) \\ \vec{J}_\rho = \tilde{k}\rho(\tilde{c},\varphi_n)\operatorname{grad}\varphi_{\mathrm{n}} & \text{in } \Omega \quad (20) \\ \vec{J}_\rho\cdot\vec{n} = \tilde{k}\rho f_{2n} & \text{on } \Gamma_{n2} \quad (21) \\ \varphi_n = f_{2n} & \text{on } \Gamma_{d2} \quad (22) \end{cases}$$

f_{1d} and f_{1n} are given boundary conditions on $\tilde{c}$ (respectively of Dirichlet and Neumann type), and f_{2d} and f_{2n} similarly for φ_n.

The system we have to consider is now made up of four equations (15) (16) (19) (20) with the four unknowns $(\tilde{c}, \vec{V}, \varphi_n, \vec{J}_\rho)$.

We consider now the following Sobolev spaces

$$H(\mathrm{div}) = \{\mathrm{w} | \mathrm{w} \in (\mathrm{L}^2(\Omega))^2, \quad \operatorname{div}\mathrm{w} \in \mathrm{L}^2(\Omega)\} \tag{23}$$

$$V_{0,i} = \{w | w \in H(\mathrm{div}), \quad \mathrm{w} \cdot \mathrm{n} = 0 \ \text{ on } \Gamma_{\mathrm{n,i}}\} \tag{24}$$

Then, for sufficiently smooth data we can obtain the following equivalent dual mixed variational formulation of the original problem.

Find $\vec{V} \in H(\mathrm{div}), \quad \tilde{\mathrm{c}} \in \mathrm{L}^2(\Omega)$
$\vec{J}_\rho \in H(\mathrm{div}), \quad \varphi_{\mathrm{n}} \in \mathrm{L}^2(\Omega)$ such that

$$\begin{cases} -\displaystyle\int_\Omega \mathrm{div}\, \vec{V} \cdot v_1 \, dx - \int_\Omega \tilde{\alpha}\rho(\tilde{c}, \varphi_n) \cdot v_1 \, dx = 0 \quad \forall v_1 \in L^2(\Omega) & (25) \\ \displaystyle\int_\Omega [D_c]^{-1} \vec{V} \cdot \vec{w}_1 \, dx + \int_\Omega \tilde{c} \cdot \mathrm{div}\, \vec{w}_1 \, dx - \int_{\Gamma_{d1}} f_{1d} \cdot \vec{w}_1 \cdot \vec{n} \, d\Gamma = 0 \quad \forall \vec{w}_1 \in V_{0,1} & (26) \\ \vec{V} \cdot \vec{n} = D_c \, f_{1n} \ \text{ on } \Gamma_{n,1} & (27) \end{cases}$$

$$\begin{cases} \displaystyle\int_\Omega \frac{\partial \rho(\tilde{c}, \varphi_n)}{\partial t} \cdot v_2 \, dx - \int_\Omega \mathrm{div}\, \vec{J}_\rho \cdot v_2 \, dx = 0 \quad \forall v_2 \in L^2(\Omega) & (28) \\ \displaystyle\int_\Omega [\tilde{k}\rho(\tilde{c}, \varphi_n)]^{-1} \vec{J}_\rho \cdot \vec{w}_2 \, dx + \int_\Omega \varphi_n \cdot \mathrm{div}\, \vec{w}_2 \, dx - \int_{\Gamma_{d2}} f_{2d} \cdot \vec{w}_2 \cdot \vec{n} \, d\Gamma = 0 \quad \forall \vec{w}_2 \in V_{0,2} & (29) \\ \vec{J}_\rho \cdot \vec{n} = \tilde{k}\rho(\tilde{c}, \varphi_n) \cdot f_{2n} \ \text{ on } \Gamma_{n,2} & (30) \end{cases}$$

For the numerical applications (as often it happens) we will have $f_{1n} \equiv f_{2n} \equiv 0$ so that we look for $\vec{V}$ and $\vec{J}_\rho$ in $V_{0,1}$ and $V_{0,2}$ respectively.

As in [9][12][13][14] the previous formulation (25)–(27) and (28)–(30) allows us to realize easily a discrete approximation via mixed finite elements.

We retain the lowest order M.F.E. of Raviart-Thomas (R_0^T) for implementation. After a triangulation $\mathcal{T}_h$ of the computational domain $\Omega \subset \mathbb{R}$, we define the following finite dimensional spaces

$$L_h = \{v_h \in L^2(\Omega) | \forall K \in \mathcal{T}_h, \quad v_h|_K = \ \text{constant}\} \quad , \tag{31}$$

$$V_h = \{w_h \in H(\mathrm{div}) | \forall \mathrm{K} \in \mathcal{T}_\mathrm{h}, \quad \mathrm{w_h(x,y)}|_\mathrm{K} = \left|{}^{\alpha_\mathrm{K}}_{\beta_\mathrm{K}} + \gamma_\mathrm{K}\right|^{\mathrm{x}}_{\mathrm{y}}\}. \tag{32}$$

We assume also that $\Gamma_{n,i}$ $(i = 1, 2)$ is obtained by union of edges of triangles which belong to the mesh $\mathcal{T}_h$ and that

$$V_{0,i,h} = V_{0,i} \cap V_h. \tag{33}$$

Then the discrete formulation of the problem follows directly from (25)–(30) by replacing $L^2(\Omega)$ by L_h and $V_{0,i}$ by $V_{0,i,h}$.

3.2 Solution algorithm

Refering again to the publications related to semiconductor area [9][11][12] [13][14], various algorithms are described for a "stationary" version of system (25)–(30) (i.e. without $\frac{\partial \rho}{\partial t}$ term !). Let us recall here the major characteristics of these numerical schemes.

• association to each (stationary) equation (primal variable) of the system of an "artificial" transient equation,

• semi-implicit (Peaceman Rachford, Douglas Rachford) or implicit (Backward-Euler) time discretization schemes for the "artificial" evolution equations. Use of local time steps,

• relaxation on the equations at each time step,

• for each time step, and for each equation of the system, solution of the nonlinear problem by Newton-Raphson technique.

The fact that we associate an "evolution" equation and the use of implicit or semi-implicit schemes is an other way to consider augmented Lagrangian techniques for the solution of saddle point problems [15] arising from the mixed formulation. Local time steps are closely connected with the penalty functions in the framework of Augmented Lagrangian techniques.

Special features of such an approach are relative simplicity and ease of implementation of model extensions. It is easy to add one equation to the system without need of deep changes in the algorithm architecture. Equations are handled successively in the algorithmic process. This numerical scheme, specially when using backward Euler for time discretization, has appeared to be rather efficient for semiconductor device (drift diffusion model and standard applied potentials). One can think reasonably that if the coupling between the equations of the system is not "too strong" then the relaxation on the equations do not penalize strongly the (speed of) convergence of the iterates towards the stationary solution of the whole system. This is certainly what happens in the static drift diffusion model for regimes not so far from the equilibrium state.

Nevertheless this solution technique failed when applied to energy-transport models for semiconductors [6] [7]. One equation (relative to electron temperature) has been added to the drift diffusion model and the constitutive relation for the current density has been slightly modified. The previous numerical scheme works correctly only for solutions very close to the equilibrium state. In order to recover the algorithmic behaviour, for typical load range, similar to the behaviour, obtained when using the drift diffusion model, one has to consider simultaneously (couple) the equations relative to the electron current continuity and the energy [7]. The implementation of such numerical scheme in a little bit more complicated but seems a necessity to insure the convergence of the iterative procedure.

In past few years we are also interested by the numerical simulation of the transient behaviour (physical transient) of a semiconductor device governed by the drift diffusion model (numerical simulation of the switching of a diode). The model is very close to the "chemotaxis model".

After the semi-discretization in time, using fully implicit scheme, we have to deal with a sequence of "quasi-static" problems which are similar to the static drift diffusion problem himself, but generally easier to solve because the nonlinearities involved are of lower amplitude. The degree of nonlinearity may be controlled in practice by the physical time step. For "very small time step" the operator governing the transient tends to the identity operator (linear operator) and for sufficiently large time steps, the operator corresponds to the static drift diffusion (fully non linear operator).

The first attempt for the numerical simulation of the transient behaviour was to apply the most efficient scheme developped for the static drift diffusion model at each "quasi static" problem obtained via the semi-discretization in time of the transient model. As the time step (physical time step) becomes smaller and smaller the convergence of the iterates becomes more and more difficult to obtain and solution of quasi-static problems is not reached. The whole algorithm failed to converge. The only plausible explanation to this algorithm behaviour is that, as the time step (physical time step) becomes smaller, the coupling between the equations (Poisson equation

and continuity equations) becomes stronger, and the relaxation strategy (decoupling) used in the numerical algorithm is no more adapted. A more implicit scheme has to be used for the solution of the quasi-static problems. The fully implicit scheme (on the system and not on each equation of the system) has been implemented and convergence was restored.

We describe now an adaptation of this numerical scheme as simply as possible.

A) Semi-discretization in time (physical time), by a fully implicit scheme (Backward-Euler)

The solution of the problem represents an approximation of the transient solution at different times $T_{n+1} = T_n + \delta t$ $(n = 0, 1, 2, 3, ...)$; the time step δt may be adapted if needed. The formulation of the sequence of quasi-static problems is the following:

Find $(\tilde{c}^{n+1}, \vec{V}^{n+1}, \varphi_n^{n+1}, \vec{J}_\rho^{n+1})$ solution of

$$-\operatorname{div} \vec{V}^{n+1} - \tilde{\alpha}\rho(\tilde{c}^{n+1}, \varphi_n^{n+1}) = 0 \tag{34}$$

$$\int_\Omega [D_c]^{-1}\vec{V}^{n+1} \cdot w_1 \, dx + \int_\Omega c^{n+1} \operatorname{div} w_1 \, dx - \int_{\Gamma_{d1}} f_{1d}\, w_1 \cdot n \, d\Gamma = 0, \quad \forall w_1 \in V_{0,1,h} \tag{35}$$

$$-\operatorname{div} \vec{J}_\rho + \frac{1}{\delta t}\left[\rho(\tilde{c}^{n+1}, \varphi_n^{n+1}) - \rho(\tilde{c}^n, \varphi_n^n)\right] = 0 \tag{36}$$

$$\int_\Omega [\tilde{k}\rho(\tilde{c}^{n+1}, \varphi_n^{n+1})]^{-1}\vec{J}_\rho \cdot w_2 \, dx + \int_\Omega \varphi_n^{n+1} \cdot \operatorname{div} w_2 \, dx - \int_{\Gamma_{d2}} f_{2d}\, w_2 \cdot n \, d\Gamma = 0, \quad \forall w_2 \in V_{0,2,h}. \tag{37}$$

B) Each quasi-static problem (index n) is solved via artificial transient [12][14]. The index of time discretization is here k (Backward Euler scheme on the system of equation)

$$\tilde{c}^{k+1} - \tilde{c}^k - \Delta t_1(x) \operatorname{div} \vec{V}^{k+1} - \Delta t_1(x) \cdot \tilde{\alpha}\rho(\tilde{c}^{k+1}, \varphi_n^{k+1}) = 0 \tag{38}$$

$$\int_\Omega [D_0]^{-1}\vec{V}^{k+1} \cdot w_1 \, dx + \int_\Omega c^{k+1} \operatorname{div} w_1 \, dx - \int_{\Gamma_{d1}} f_{1d}\, w_1 \cdot n \, d\Gamma = 0, \quad \forall w_1 \in V_{0,1,h} \tag{39}$$

$$\varphi_n^{k+1} - \varphi_n^k - \Delta t_2(x) \operatorname{div} \vec{J}_\rho^{k+1} + \Delta t_2(x) \cdot \frac{1}{\partial t}[\rho(\tilde{c}^{k+1}, \varphi_n^{k+1}) - \rho^n] = 0 \tag{40}$$

$$\int_\Omega [\tilde{k}\rho(\tilde{c}^{k+1}, \varphi_n^{k+1})\vec{J}_\rho^{k+1} \cdot w_2 \, dx + \int_\Omega \varphi_n^{k+1} \cdot \operatorname{div} w_2 \, dx - \int_{\Gamma_{d2}} f_{2d}\, w_2 \cdot n \, d\Gamma = 0, \quad \forall w_2 \in V_{0,2,h} \tag{41}$$

In (40) ρ^n is given $(\rho^n = \rho(\tilde{c}^n, \varphi_n^n))$; In this process indexed with k, we can take $\tilde{c}^0 = \tilde{c}^n$ and $\varphi_n^0 = \varphi_n^n$. The unknowns are here $(\tilde{c}^{k+1}, \vec{V}^{k+1}, \varphi_n^{k+1}, \vec{J}_\rho^{k+1})$. When the convergence with respect to k is obtained, then the current solution gives $(\tilde{c}^{n+1}, \vec{V}^{n+1}, \varphi_n^{n+1}, \vec{J}_\rho^{n+1})$.

As we use the lowest order Raviart-Thomas element, the equations (38) and (40) lead to scalar relation on each elements T of the triangulation $\mathcal{T}_h$ (it is natural in this approximation to take the "local time steps" Δt_1 and Δt_2 constant on each element T).

C) At each step k, we have a non linear problem to solve. We use Newton-Raphson technique, the index of iteration is now denoted by ℓ. We set:

$$\vec{U} = \begin{pmatrix} \tilde{c} \\ \vec{V} \\ \varphi_n \\ \vec{J}_\rho \end{pmatrix} = \begin{pmatrix} U_1 \\ U_2 \\ U_3 \\ U_4 \end{pmatrix} \tag{42}$$

Equations (38) and (39) can formally be written as

$$E_1(\tilde{c}, \vec{V}, \varphi_n, \cdot) = E_1(U_1, U_2, U_3, U_4) = E_1(\vec{U}) = 0.$$

$$E_2(\tilde{c}, \vec{V}, \cdot, \cdot) = E_2(U_1, U_2, U_3, U_4) = E_2(\vec{U}) = 0$$

and so on, and finally the system (38)–(41) may be synthetized by

$$\vec{E}(\vec{U}) = 0. \tag{43}$$

The Newton-Raphson rule applied to (43) gives

$$\left[\frac{\partial E_i}{\partial U_j}\right]_\ell \delta\vec{U}^\ell = -\vec{E}(\vec{U})^\ell, \quad \delta\vec{U}^\ell = \vec{U}^{\ell+1} - \vec{U}^\ell \tag{44}$$

or equivalently

$$\vec{U}^{\ell+1} = \vec{U}^\ell - \left[\frac{\partial E_i}{\partial U_j}\right]_\ell^{-1} \vec{E}(\vec{U})^\ell \tag{45}$$

where $\left[\frac{\partial E_i}{\partial U_j}\right]_\ell$ is the jacobian matrix of the application $\vec{E}$ evaluated at step ℓ.

The Newton-Raphson technique leads to a sequence of linear systems (indexed by ℓ). In our context of approximation (M.F.E.-RT_0) the size of each linear system is approximatively

$$2 \times (NT + NA)$$

where NT is the number of triangles of the triangulation $\mathcal{T}_h$, and NA is the number of edges of the mesh.

On can reduce the size of linear system by eliminating the primal variables (i.e., $\tilde{c}$ and φ_n).

As a matter of fact, if we consider the first and third rows of relation (44), we can express explicitely the primal variables $(\tilde{c}^{\ell+1}, \varphi_n^{\ell+1})$ as functions of the dual variables $\vec{V}^{\ell+1}$ and $\vec{J}_\rho^{\ell+1}$ by

$$[A] \begin{bmatrix} \tilde{c}^{\ell+1} - \tilde{c}^\ell \\ \varphi_n^{\ell+1} - \varphi_n^\ell \end{bmatrix} = \begin{bmatrix} \Delta t_1 \cdot \operatorname{div} \delta\tilde{\mathrm{V}}^\ell \\ \Delta t_2 \operatorname{div} \delta\tilde{\mathrm{J}}_\rho^\ell \end{bmatrix} - \begin{bmatrix} E_1(\vec{U}^\ell) \\ E_3(\vec{U}^\ell) \end{bmatrix}. \tag{46}$$

The matrix $[A]$ is given by

$$[A] = \begin{bmatrix} 1 - \Delta t_1 \tilde{\alpha} \rho'_{\tilde{c}}\big|_\ell & -\Delta t_1 \tilde{\alpha} \rho'_{\varphi_n}\big|_\ell \\ \dfrac{\Delta t_2}{\delta t} \rho'_{\tilde{c}}\big|_\ell & 1 + \dfrac{\Delta t_2}{\delta t} \rho'_{\varphi_n}\big|_\ell \end{bmatrix}. \tag{47}$$

By the definition of ρ in (11), the derivatives of ρ with respect to $\tilde{c}$ and φ_n are the same and the determinant of A can be evaluated as

$$\det \mathrm{A} = 1 + \rho'_{\tilde{\mathrm{c}}} \left(\frac{\Delta \mathrm{t}_2}{\delta \mathrm{t}} - \Delta \mathrm{t}_1 \cdot \tilde{\alpha} \right). \tag{48}$$

We can eventually act on the physical time step δt or the local time steps Δt_1 and Δt_2 in order to keep $\det \mathrm{A} \neq 0$ or even > 0.

Let us denote by B the inverse of matrix A

$$B = A^{-1}. \tag{49}$$

Then the following relations are obtained for $\tilde{c}^{\ell+1}$ and $\varphi_n^{\ell+1}$

$$\left.\begin{aligned} \tilde{c}^{\ell+1} - \tilde{c}^{\ell} = \delta\tilde{c}^{\ell} &= B_{11}\Delta t_1 \,\mathrm{div}\,\tilde{\mathrm{V}}^{\ell+1} - \mathrm{B}_{11}[\tilde{\mathrm{c}}^{\ell} - \tilde{\mathrm{c}}^{\mathrm{k}} - \Delta\mathrm{t}_1\tilde{\alpha}\rho^{\ell}] \\ &+ B_{12}\Delta t_2 \,\mathrm{div}\,\tilde{\mathrm{J}}_{\rho}^{\ell+1} - \mathrm{B}_{12}\left[\varphi_{\mathrm{n}}^{\ell} - \varphi_{\mathrm{n}}^{\mathrm{k}} + \frac{\Delta\mathrm{t}_2}{\delta\mathrm{t}}\left(\rho^{\ell} - \rho^{\mathrm{n}}\right)\right] \end{aligned}\right\} \tag{50}$$

$$\left.\begin{aligned} \varphi_n^{\ell+1} - \varphi_n^{\ell} = \delta\varphi_n^{\ell} &= B_{21}\Delta t_1 \,\mathrm{div}\,\tilde{\mathrm{V}}^{\ell+1} - \mathrm{B}_{21}[\tilde{\mathrm{c}}^{\ell} - \tilde{\mathrm{c}}^{\mathrm{k}} - \Delta\mathrm{t}_1\tilde{\alpha}\rho^{\ell}] \\ &+ B_{22}\Delta t_2 \,\mathrm{div}\,\tilde{\mathrm{J}}_{\rho}^{\ell+1} - \mathrm{B}_{22}\left[\varphi_{\mathrm{n}}^{\ell} - \varphi_{\mathrm{n}}^{\mathrm{k}} + \frac{\Delta\mathrm{t}_2}{\delta\mathrm{t}}\left(\rho^{\ell} - \rho^{\mathrm{n}}\right)\right]. \end{aligned}\right\} \tag{51}$$

These relations (50) and (51) are then used within the second and fourth rows of (45). Finally the linear system we have to solve is relative to the unknowns $\vec{V}^{\ell+1}$ and $\vec{J}_{\rho}^{\ell+1}$ only (i.e. of maximum size $2.NA$). When the convergence with respect to ℓ is reached then the solution at step k of the whole process is obtained.

4 Numerical Applications

We take for Ω the rectangular domain $L \times \ell$ and we suppose that at $T = 0$ we have a uniform

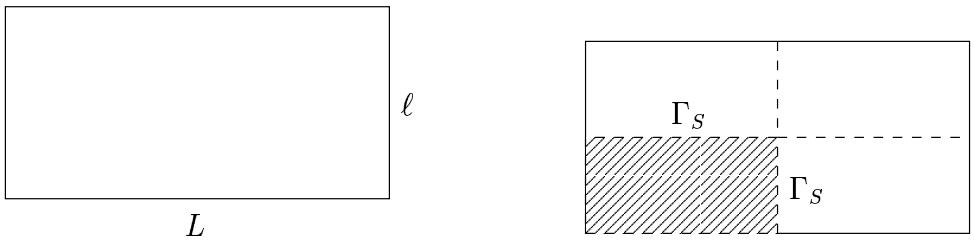

Figure 1: *Simulation Domain and reduction by symmetry.*

distribution of bacteria with density ρ_0.

From the definition of ρ in (11) it is natural to take at initial time

$$\tilde{c} + \varphi_n = 0. \tag{52}$$

By analogy with the drift diffusion model for semiconductor the variable $\tilde{c}$ is similar to the electrostatic potential which is defined up to an additive constant. We can fix this constant by taking the value 0. On the other hand we want to ensure in the following numerical approximation, the mass conservation (or volume conservation) for the bacteria. From eq. (13) this will be the case if we take the following boundary condition on φ_n

$$\frac{\partial\varphi_n}{\partial n} = 0 \quad \text{on } \Gamma = \partial\Omega. \tag{53}$$

In short, we can take at initial time

$$\rho = \rho_0 \text{ and } \tilde{c} = \varphi_n \equiv 0 \tag{54}$$

and the boundary condition

$$\left.\begin{aligned} \tilde{c}|_\Gamma &= 0 \\ \frac{\partial \varphi_n}{\partial n}\Big|_\Gamma &= 0 \end{aligned}\right\} \tag{55}$$

Of course, by reason of symmetry we can consider only a quarter of the simulation domain Ω, namely $(L/2, \ell/2)$, then we have to take the following boundary conditions on the boundaries of symmetry Γ_S

$$\left.\begin{aligned} \frac{\partial \tilde{c}}{\partial n} &= 0 \quad \text{on } \Gamma_S, \\ \text{and } \frac{\partial \varphi_n}{\partial n} &= 0 \quad \text{on } \Gamma_S. \end{aligned}\right\} \tag{56}$$

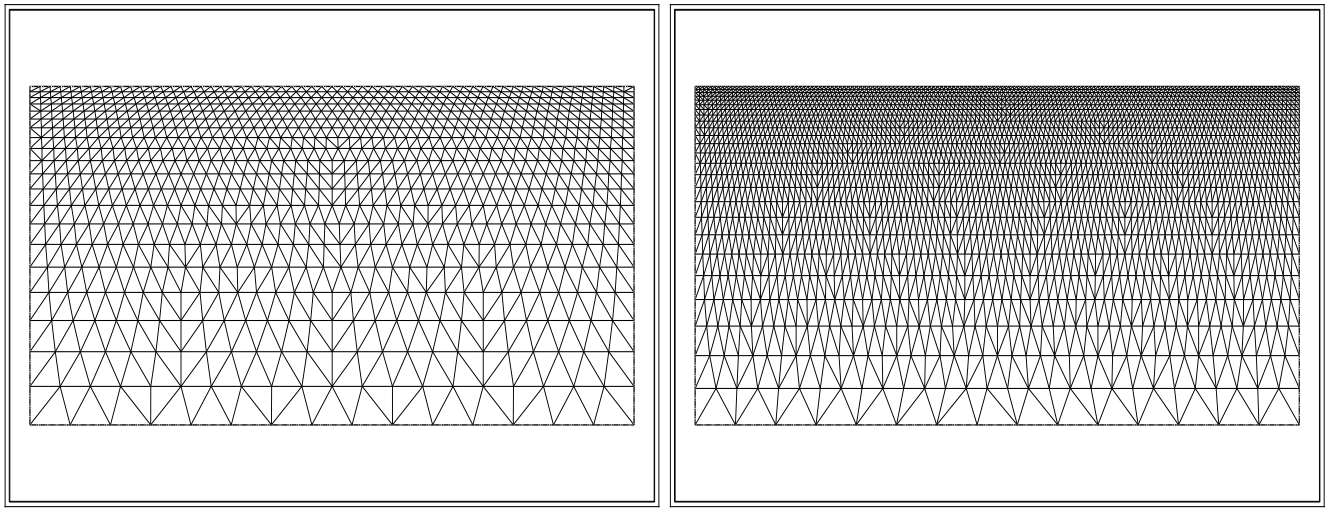

(a) Mesh 1 (1775 triangles) (b) Mesh 2 (5433 triangles)

Figure 2: MESHES. *The meshes are adapted to the geometries by deformation .*

In all numerical experimentations, two meshes have been used in order to see if the transient may be strongly affected by the spatial discretization. Fig (2) show the first mesh (with 1775 triangles) and the second mesh (with 5433 triangles)

The bacterial density is also assumed to be larger than a prescribed minimum value ρ_{min} (projection). We choose in our simulations,

$$\rho_{min} = 10^{-10}/cm^3. \tag{57}$$

4.1 Numerical results with Ω = square

In this part, we take $L = \ell = 0.5cm$;

The physical parameters are those given in section 1. The model for attractant diffusion and production is given by (4). In (8) the scaling factor q is taken (as in other applications) as 10^{-12}. The initial uniform distribution of bacteria is taken $\rho_0 = 10^6/cm^3$.

The figures(3,4) represent the distribution of bacteria density within the domain of simulation at times $100s$ and $2000s$ and for the two meshes. The coordinates (x_1, x_2) are given in μm on the figures and a log scale is used for representation of the density ρ (range from 10^{-10} to 10^{+10} (cm^{-3})). The initial constant value ρ_0 is marked on the figures.

The total amount of bacteria remain constant along the evolution process:

$$\int_\Omega \rho \, dx = C^{te} = \int_\Omega \rho_0 \, dx = \rho_0 \times Area(\Omega)$$

For this example, the bacteria migrate towards the center of the square. Something like a Dirac mass at this center is obtained after a certain amount of time (see fig.(4)) A P^1-smoothing is applied (for visualization of solution) to the raw data obtained from the mixed finite element approximation. The primal variables $\tilde{c}, \varphi_n$ and associated quantities (as bacteria density) are constant on each triangle of the mesh. As such an action (smoothing) reduce strongly the function peaks, a special treatment (only for visualization) is applied on the smoothed function in order to retrieve peak values.

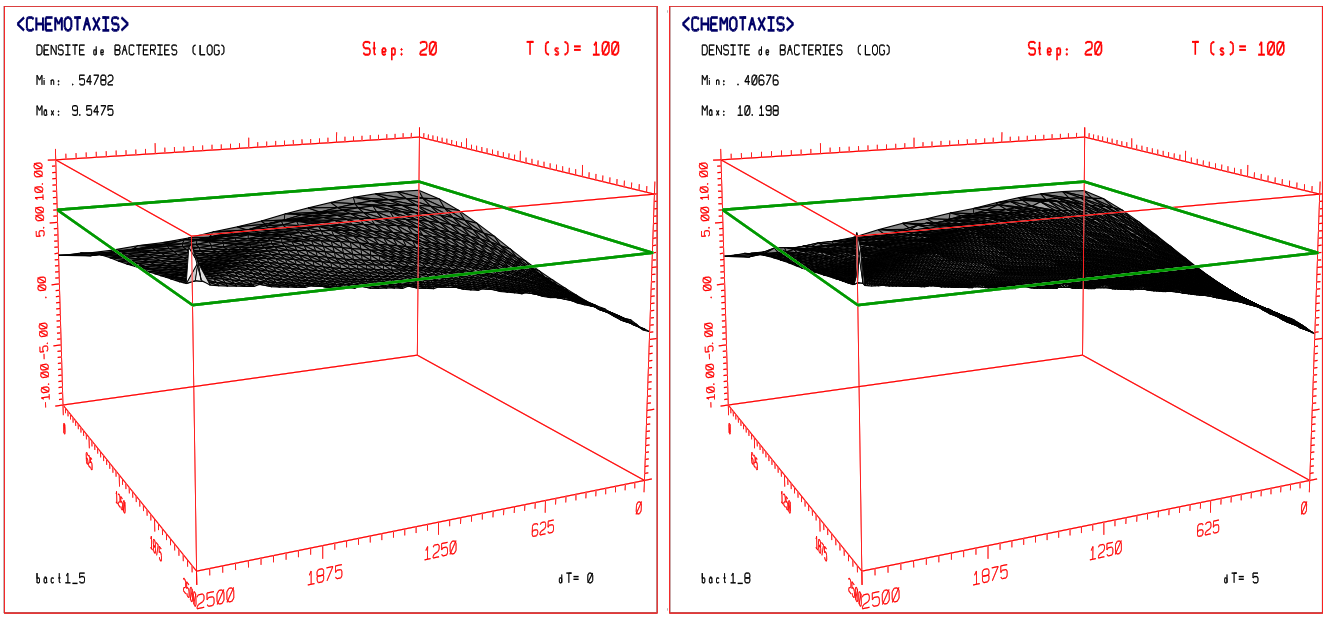

(a) With mesh 1 (1775 triangles)

(b) With mesh 2 (5433 triangles)

Figure 3: Bacteria concentration, (Log. scale). *Computational domain:square* $0.25cm \times 0.25cm$. *Distribution after 100s. Initial Concentration is marked, observer position near* (x_{max}, y_{max}).

In order to follow quantitatively what happens to the bacterial density distribution, we can analyse the solution at a given time T in the following way:

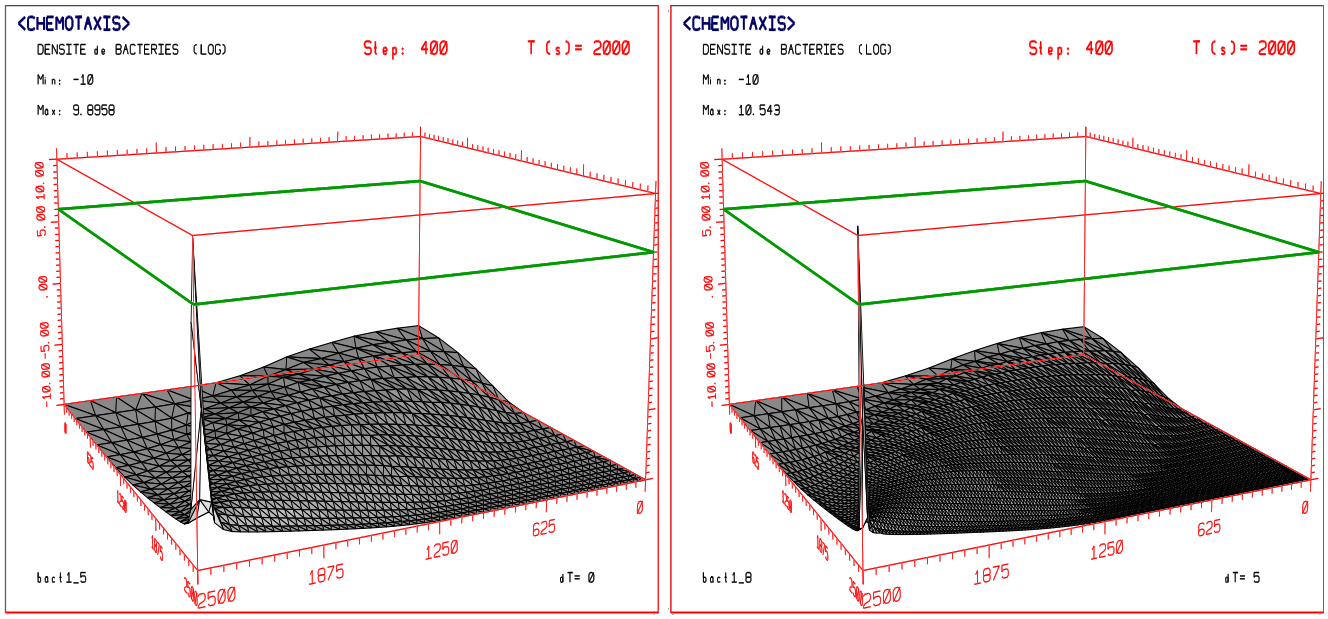

(a) With mesh 1 (1775 triangles)

(b) With mesh 2 (5433 triangles)

Figure 4: Bacteria concentration, (Log. scale). *Computational domain:square* $0.25cm \times 0.25cm$. *Distribution after 2000s. Initial Concentration is marked, observer position near* (x_{max}, y_{max}).

1. We control the value of the total bacterial mass (which remains constant during the evolution process)

$$Total\_Mass = \int_\Omega \rho \, dx = \sum_J \rho(J) * Area(J) \quad (J \text{ triangle of the mesh})$$

2. We consider a threshold value (ρ_{th} -typically we choose $\rho_{th} = \rho_0$-) for the density ρ and only triangles for which the density is larger or equal than ρ_{th} will be taken into consideration in the following. First of all, we begin to attach the attribute *"not marked"* to all the triangles.

3. -Determination of the i^{th} local maxima

   - We look for the triangle J_i such that

$$\rho(J_i) \geq \rho(J) \quad \forall J$$

     where $J \in$ list of *"not marked"* triangles and such that $\rho(J) \geq \rho_{th}$
   - If the triangle J_i does not exists $\Longrightarrow EXIT$ (GoTo END)
   - The triangle J_i is *"marked"*
   - We determine all the triangles $J_{i,k}$ in the (connected) neighbourhood of J_i such that
     - $\rho(J_{i,k}) \geq \rho_{th}$
     - $J_{i,k}$ *"not marked"*

All these triangles $J_{i,k}$ (including J_i) form a connected domain Ω_i

$$\Omega_i = J_i \bigcup_k J_{i,k}$$

- We evaluate and print several quantities
  - J_i = number of the triangle where the local maximun(i) occur
  - $Conc$ = density value (local maximum)
  - $XG(J_i), YG(J_i)$ = coordinates of the center of gravity for triangle J_i
  - $N(i)$ = number of triangles in Ω_i
  - $Local\_Mass(i) = \int_{\Omega_i} \rho \, dx$
  - $Contrib(J_i) = \rho(J_i) \times Area(J_i)$
  - $Percent(i) = \frac{Local\_Mass(i)}{Total\_Mass} \times 100$
  - $Percent\_max\_local(i) = \frac{Contrib(J_i)}{Local\_Mass(i)} \times 100$
  - $Percent\_max\_total(i) = \frac{Contrib(J_i)}{Total\_Mass} \times 100$
- All triangles in Ω_i are *"marked"*
- Return to 3 for the determination of next local max.
- END
  - At this point, a certain number (I) of local maxima has been found
    - N = the total number of triangles considered = $\sum_i N(i)$
    - $Troncated\_Mass = \sum_i Local\_Mass(i)$
    - $Troncated\_Mass\_Percent = \frac{Troncated\_Mass}{Total\_Mass} \times 100$

Analysis of the solution on Mesh 2 at $100s$ and $2000s$

```
------------------------------------------------ Mesh 2
... Process time :   100.0 s  Total bacteria mass: 6.25000E+04    Threshold value: 1.00000E+06
---------------------------  Local max number: 1
*** J1 =  5433    Conc: 1.577E+10  (XG,YG)= ( 2.489E-01, 2.493E-01) (cmXcm)
    Number of triangles  N(1)=   1532
    Local_Mass(1)  =  5.26292E+04 Percent(1)          =  84.20681 %
    Contrib(  5433)=  2.82386E+04 Percent_max_local(1)=  53.65572 %    Percent_max_total(1)=  45.18177 %
 -------- Global results ------
    Number of local maxima : 1  Total number of triangles  N=  1532
    Troncated_Mass : 5.26292E+04  Troncated_Mass_Percent : 84.20681 %

------------------------------------------------ Mesh 2
... Process time :  2000.0 s  Total bacteria mass: 6.25001E+04    Threshold value: 1.00000E+06
---------------------------  Local max number: 1
*** J1 =  5433    Conc: 3.490E+10  (XG,YG)= ( 2.489E-01, 2.493E-01) (cmXcm)
    Number of triangles  N(1)=      1
    Local_Mass(1)  =  6.25001E+04 Percent(1)          =  99.99998 %
    Contrib(  5433)=  6.25001E+04 Percent_max_local(1)= 100.00000 %    Percent_max_total(1)=  99.99998 %
 -------- Global results ------
    Number of local maxima : 1  Total number of triangles  N=     1
    Troncated_Mass : 6.25001E+04  Troncated_Mass_Percent : 99.99998 %
```

We can see (qualitatively) on figure (4) the formation of a Dirac Mass at the center of the square. Quantitatively, we can see from the solution analysis at $600s$ that only one triangle (the smallest part in our MFE approximation) contribute to the total Mass. As early as the process time reached $100s$, this triangle contained more than 45% of the total mass of bacteria.

4.2 Numerical results with Ω = rectangle with small aspect ratio

In this part, we take $L = 1.cm \quad \ell = 0.5cm$;

The figures(5,6) represent the distribution of bacteria density within the domain of simulation at times $100s$ and $600s$ and for the two meshes.

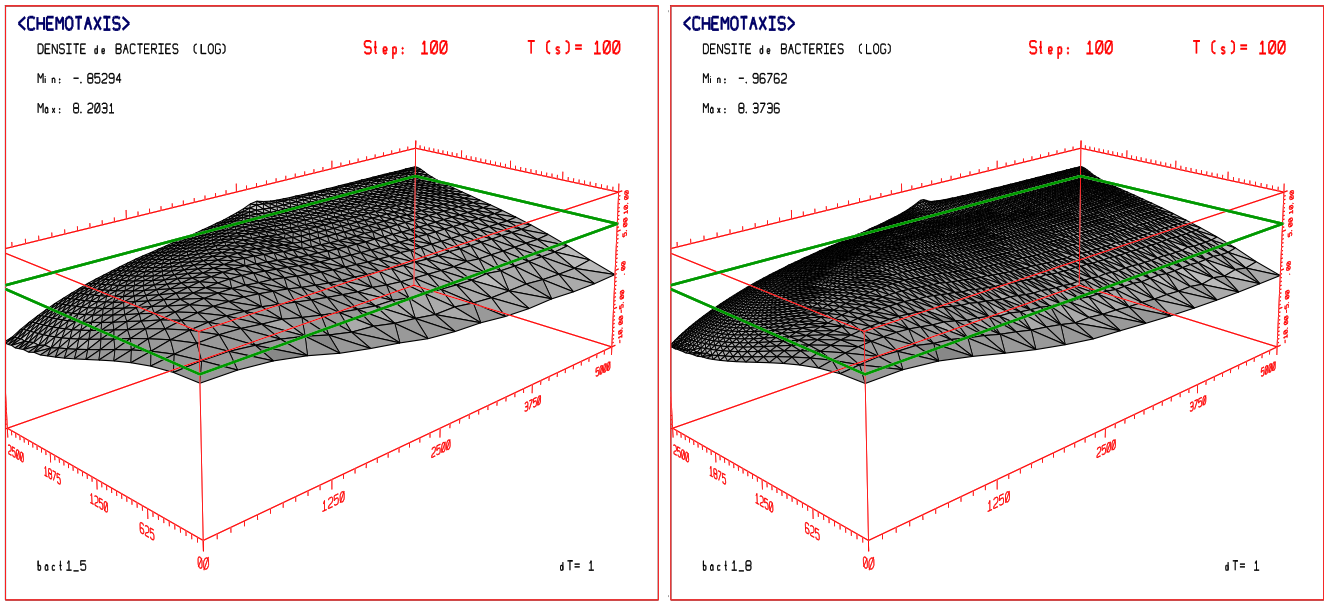

(a) With mesh 1 (1775 triangles) (b) With mesh 2 (5433 triangles)

Figure 5: Bacteria concentration,(Log. scale). *Computational domain:rectangle* $0.50cm \times 0.25cm$. *Distribution after 100s. Initial Concentration is marked, observer position near* (x_{min}, y_{min}).

Analysis of the solution on meshes 1 and 2 at time 100s

```
------------------------------------------------ Mesh 1
... Process time :   100.0 s  Total bacteria mass: 1.25000E+05    Threshold value: 1.00000E+06
----------------------------  Local max number: 1
*** J1 =  1115    Conc: 1.597E+08  (XG,YG)= ( 2.710E-01, 2.487E-01) (cmXcm)
    Number of triangles  N(1)=    605
    Local_Mass(1)  =  1.11694E+05 Percent(1)          =  89.35488 %
    Contrib(  1115)=  2.55813E+03 Percent_max_local(1)=   2.29031 %    Percent_max_total(1)=   2.04651 %
 -------- Global results ------
    Number of local maxima : 1  Total number of triangles  N=   605
    Troncated_Mass : 1.11694E+05  Troncated_Mass_Percent : 89.35488 %

------------------------------------------------ Mesh 2
... Process time :   100.0 s  Total bacteria mass: 1.25000E+05    Threshold value: 1.00000E+06
----------------------------  Local max number: 1
*** J1 =  3372    Conc: 2.365E+08  (XG,YG)= ( 2.746E-01, 2.493E-01) (cmXcm)
    Number of triangles  N(1)=   2107
    Local_Mass(1)  =  1.11937E+05 Percent(1)          =  89.54935 %
    Contrib(  3372)=  8.46726E+02 Percent_max_local(1)=   0.75643 %    Percent_max_total(1)=   0.67738 %
 -------- Global results ------
    Number of local maxima : 1  Total number of triangles  N=  2107
    Troncated_Mass : 1.11937E+05  Troncated_Mass_Percent : 89.54935 %
```

Analysis of the solution on meshes 1 and 2 at time 600s

```
------------------------------------------------ Mesh 1
... Process time :   600.0 s  Total bacteria mass: 1.25000E+05    Threshold value: 1.00000E+06
```

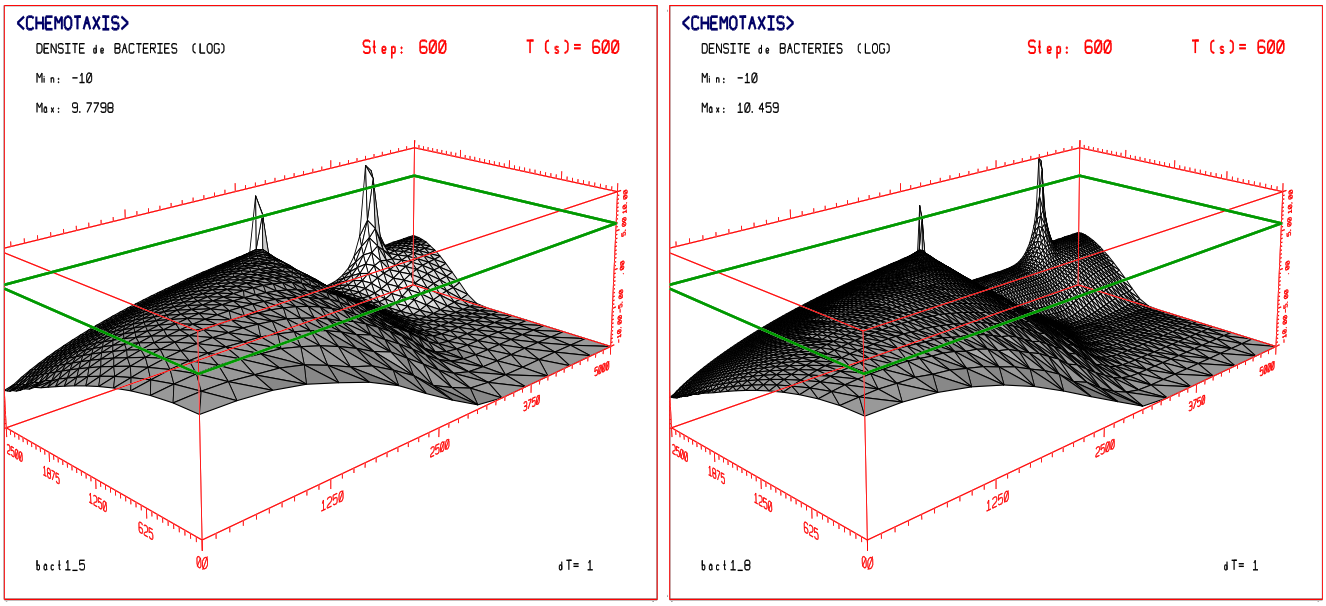

(a) With mesh 1 (1775 triangles)

(b) With mesh 2 (5433 triangles)

Figure 6: Bacteria concentration, (Log. scale). *Computational domain:rectangle* $0.50cm \times 0.25cm$. *Distribution after 600s. Initial Concentration is marked, observer position near* (x_{min}, y_{min}).

```
----------------------------  Local max number: 1
*** J1 =  1146    Conc: 6.023E+09  (XG,YG)= ( 2.794E-01, 2.487E-01) (cmXcm)
    Number of triangles  N(1)=      1
    Local_Mass(1)  =  9.64805E+04 Percent(1)          =  77.18437 %
    Contrib(  1146)=  9.64805E+04 Percent_max_local(1)= 100.00000 %    Percent_max_total(1)=  77.18437 %
----------------------------  Local max number: 2
*** J2 =  1636    Conc: 1.780E+09  (XG,YG)= ( 4.302E-01, 2.487E-01) (cmXcm)
    Number of triangles  N(2)=      1
    Local_Mass(2)  =  2.85119E+04 Percent(2)          =  22.80950 %
    Contrib(  1636)=  2.85119E+04 Percent_max_local(2)= 100.00000 %    Percent_max_total(2)=  22.80950 %
 -------- Global results ------
    Number of local maxima : 2  Total number of triangles  N=     2
    Troncated_Mass : 1.24992E+05  Troncated_Mass_Percent : 99.99388 %

------------------------------------------------ Mesh 2
... Process time :   600.0 s  Total bacteria mass: 1.25000E+05    Threshold value: 1.00000E+06
----------------------------  Local max number: 1
*** J1 =  3372    Conc: 2.876E+10  (XG,YG)= ( 2.746E-01, 2.493E-01) (cmXcm)
    Number of triangles  N(1)=      1
    Local_Mass(1)  =  1.02971E+05 Percent(1)          =  82.37659 %
    Contrib(  3372)=  1.02971E+05 Percent_max_local(1)= 100.00000 %    Percent_max_total(1)=  82.37659 %
----------------------------  Local max number: 2
*** J2 =  5028    Conc: 6.145E+09  (XG,YG)= ( 4.386E-01, 2.493E-01) (cmXcm)
    Number of triangles  N(2)=      2
    Local_Mass(2)  =  2.20225E+04 Percent(2)          =  17.61800 %
    Contrib(  5028)=  2.20013E+04 Percent_max_local(2)=  99.90358 %    Percent_max_total(2)=  17.60101 %
 -------- Global results ------
    Number of local maxima : 2  Total number of triangles  N=     3
    Troncated_Mass : 1.24993E+05  Troncated_Mass_Percent : 99.99458 %
```

At $T = 100s$ we begin to see the first local maxima -see fig.(5)-, but only a few percentage of the total mass is located on the triangle which presents the maximum bacterial density. We can see on the quantitative analysis that the localization of local maxima and concentration values at

these points remain mesh dependent. We can also remark from the analysis at $T = 600s$ that the distorsion between mass repartition (at local maxima) is amplified when the mesh is refined.

4.3 Numerical results with Ω = rectangle with large aspect ratio

In this part, we take $L = 1.5cm \quad \ell = 0.5cm$;

The figures(7,8,9) represent the distribution of bacteria density within the domain of simulation at times $100s$, $250s$ and $600s$ and for the two meshes.

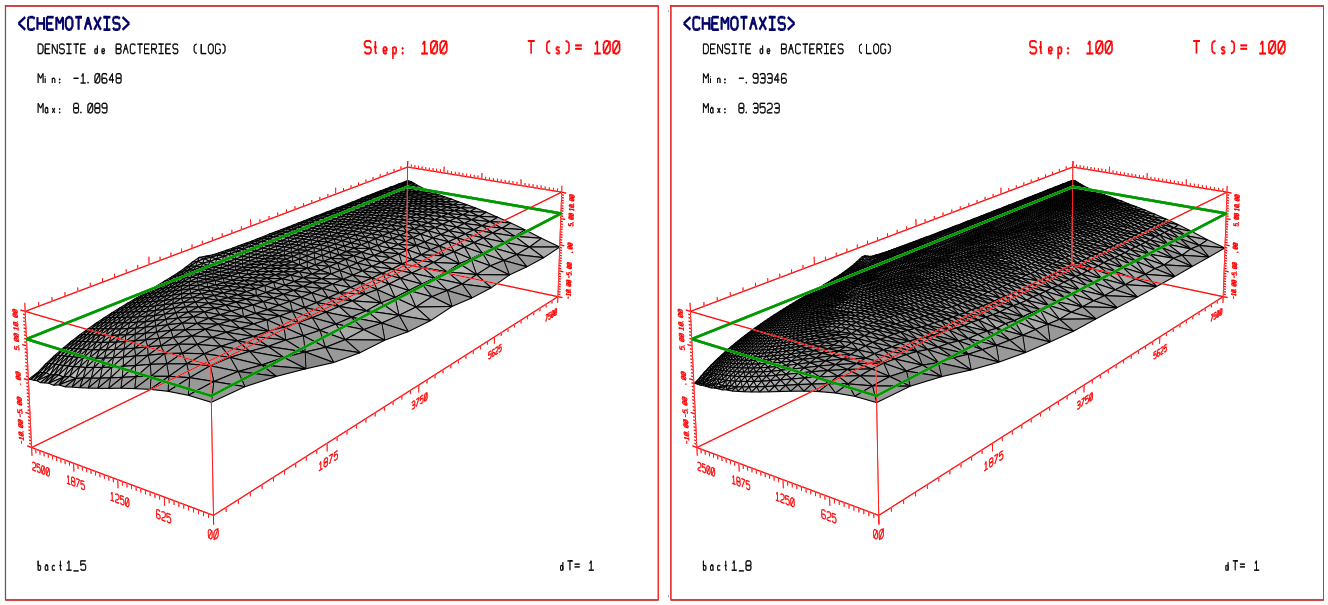

(a) With mesh 1 (1775 triangles)

(b) With mesh 2 (5433 triangles)

Figure 7: Bacteria concentration, (Log. scale). *Computational domain:rectangle* $0.75cm \times 0.25cm$. *Distribution after 100s. Initial Concentration is marked, observer position near* (x_{min}, y_{min}).

Solution analysis on mesh 1 and 2 at 100s (respectively)

```
------------------------------------------------ Mesh 1
... Process time :   100.0 s  Total bacteria mass: 1.87500E+05    Threshold value: 1.00000E+06
----------------------------  Local max number: 1
*** J1 =   830    Conc: 1.228E+08  (XG,YG)= ( 2.740E-01, 2.474E-01) (cmXcm)
    Number of triangles  N(1)=    656
    Local_Mass(1)  =  1.69660E+05 Percent(1)          =  90.48521 %
    Contrib(   830)=  3.01108E+03 Percent_max_local(1)=   1.77478 %    Percent_max_total(1)=   1.60591 %
 -------- Global results ------
    Number of local maxima : 1  Total number of triangles  N=   656
    Troncated_Mass : 1.69660E+05  Troncated_Mass_Percent : 90.48521 %

------------------------------------------------ Mesh 2
... Process time :   100.0 s  Total bacteria mass: 1.87500E+05    Threshold value: 1.00000E+06
----------------------------  Local max number: 1
*** J1 =  2500    Conc: 2.252E+08  (XG,YG)= ( 2.730E-01, 2.493E-01) (cmXcm)
    Number of triangles  N(1)=   2314
    Local_Mass(1)  =  1.69736E+05 Percent(1)          =  90.52596 %
    Contrib(  2500)=  1.20953E+03 Percent_max_local(1)=   0.71259 %    Percent_max_total(1)=   0.64508 %
 -------- Global results ------
    Number of local maxima : 1  Total number of triangles  N=  2314
    Troncated_Mass : 1.69736E+05  Troncated_Mass_Percent : 90.52596 %
```

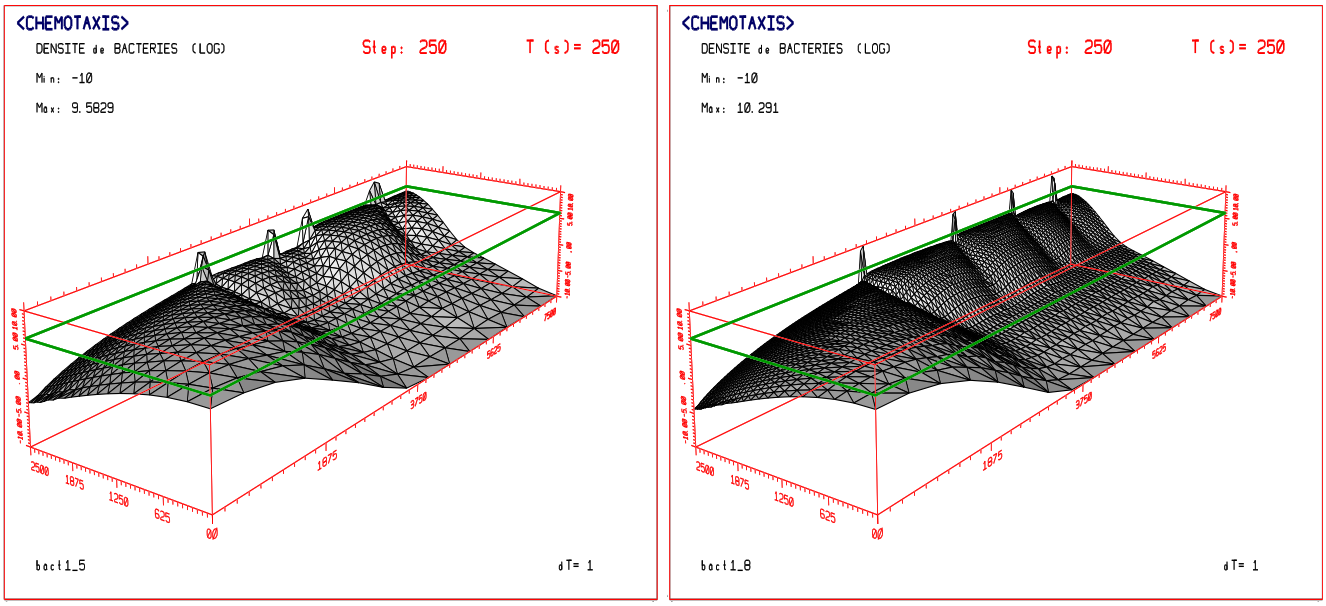

(a) With mesh 1 (1775 triangles) (b) With mesh 2 (5433 triangles)

Figure 8: Bacteria concentration, (Log. scale). *Computational domain:rectangle* $0.75cm \times 0.25cm$. *Distribution after 250s. Initial Concentration is marked, observer position near* (x_{min}, y_{min}).

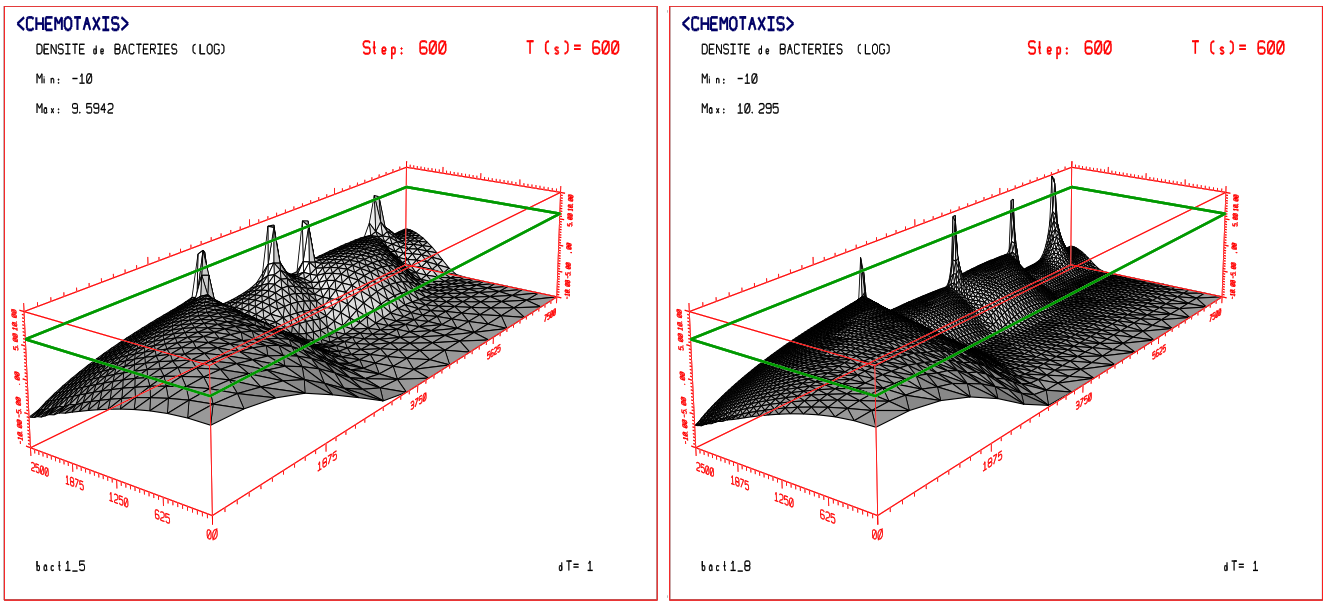

(a) With mesh 1 (1775 triangles) (b) With mesh 2 (5433 triangles)

Figure 9: Bacteria concentration, (Log. scale). *Computational domain:rectangle* $0.75cm \times 0.25cm$. *Distribution after 600s. Initial Concentration is marked, observer position near* (x_{min}, y_{min}).

Solution analysis on mesh 1 and 2 at 600s (respectively)

---------- Mesh 1

```
... Process time :   600.0 s  Total bacteria mass: 1.87500E+05    Threshold value: 1.00000E+06
---------------------------  Local max number: 1
*** J1 =   869    Conc: 3.928E+09  (XG,YG)= ( 2.808E-01, 2.487E-01) (cmXcm)
    Number of triangles  N(1)=      2
    Local_Mass(1)  =  9.71086E+04 Percent(1)          =  51.79124 %
    Contrib(   869)=  9.43845E+04 Percent_max_local(1)=  97.19479 %    Percent_max_total(1)=  50.33838 %
---------------------------  Local max number: 2
*** J2 =  1685    Conc: 1.777E+09  (XG,YG)= ( 6.704E-01, 2.487E-01) (cmXcm)
    Number of triangles  N(2)=      1
    Local_Mass(2)  =  4.26938E+04 Percent(2)          =  22.77004 %
    Contrib(  1685)=  4.26938E+04 Percent_max_local(2)= 100.00000 %    Percent_max_total(2)=  22.77004 %
---------------------------  Local max number: 3
*** J3 =  1297    Conc: 1.189E+09  (XG,YG)= ( 4.945E-01, 2.487E-01) (cmXcm)
    Number of triangles  N(3)=      1
    Local_Mass(3)  =  2.85685E+04 Percent(3)          =  15.23651 %
    Contrib(  1297)=  2.85685E+04 Percent_max_local(3)= 100.00000 %    Percent_max_total(3)=  15.23651 %
---------------------------  Local max number: 4
*** J4 =  1146    Conc: 7.957E+08  (XG,YG)= ( 4.191E-01, 2.487E-01) (cmXcm)
    Number of triangles  N(4)=      1
    Local_Mass(4)  =  1.91198E+04 Percent(4)          =  10.19721 %
    Contrib(  1146)=  1.91198E+04 Percent_max_local(4)= 100.00000 %    Percent_max_total(4)=  10.19721 %
 -------- Global results ------
    Number of local maxima : 4  Total number of triangles  N=     5
    Troncated_Mass : 1.87491E+05  Troncated_Mass_Percent : 99.99500 %

------------------------------------------------ Mesh 2
... Process time :   600.0 s  Total bacteria mass: 1.87500E+05    Threshold value: 1.00000E+06
---------------------------  Local max number: 1
*** J1 =  2500    Conc: 1.971E+10  (XG,YG)= ( 2.730E-01, 2.493E-01) (cmXcm)
    Number of triangles  N(1)=      1
    Local_Mass(1)  =  1.05869E+05 Percent(1)          =  56.46339 %
    Contrib(  2500)=  1.05869E+05 Percent_max_local(1)= 100.00000 %    Percent_max_total(1)=  56.46339 %
---------------------------  Local max number: 2
*** J2 =  4575    Conc: 5.821E+09  (XG,YG)= ( 5.927E-01, 2.493E-01) (cmXcm)
    Number of triangles  N(2)=      1
    Local_Mass(2)  =  3.12662E+04 Percent(2)          =  16.67531 %
    Contrib(  4575)=  3.12662E+04 Percent_max_local(2)= 100.00000 %    Percent_max_total(2)=  16.67531 %
---------------------------  Local max number: 3
*** J3 =  3667    Conc: 4.727E+09  (XG,YG)= ( 4.571E-01, 2.493E-01) (cmXcm)
    Number of triangles  N(3)=      1
    Local_Mass(3)  =  2.53862E+04 Percent(3)          =  13.53927 %
    Contrib(  3667)=  2.53862E+04 Percent_max_local(3)= 100.00000 %    Percent_max_total(3)=  13.53927 %
---------------------------  Local max number: 4
*** J4 =  5264    Conc: 4.649E+09  (XG,YG)= ( 6.981E-01, 2.493E-01) (cmXcm)
    Number of triangles  N(4)=      1
    Local_Mass(4)  =  2.49685E+04 Percent(4)          =  13.31652 %
    Contrib(  5264)=  2.49685E+04 Percent_max_local(4)= 100.00000 %    Percent_max_total(4)=  13.31652 %
-------- Global results ------
    Number of local maxima : 4  Total number of triangles  N=     4
    Troncated_Mass : 1.87490E+05  Troncated_Mass_Percent : 99.99449 %
```

For the present example, the two meshes give the same number of local maxima (4), but localization and relative weight to the total mass contributions are slightly different. Are the patterns too mesh sensitive? Perhaps mesh adaption may be needed in the evolution process when density gradients begin to become significants.

4.4 Numerical results with limited attactant production

The model of attractant production is given via eq. (7),

$$\alpha \rho \, e^{-\rho/\rho^\star}$$

where the parameter $\rho^\star$ is the cutoff bacterial density. For the numerical results presented in the following, we have considered only the rectangle Ω defined by $L = 1.5cm$, $\ell = 0.5cm$ and used the Mesh 2 (5433 triangles).

When taking into account the fact that the production of attractants may be bounded, the behaviour of bacterial density distribution during the process is quite different.

In the previous simulations (attractant production modelled via $\alpha\rho$), when a peak of concentration appears within the evolution process, it remains at the same (or nearly the same) place during all the process. The bacteria density decreases around these peaks.

In the present simulations, the first concentration peak travels towards the center of the domain (upper right corner of the computational domain), "eating" successively all the other local peaks of bacterial concentration. High densities values are not localized only over one mesh element.

With the values $\rho^\star = 50\rho_0$, $\rho^\star = 100\rho_0$, $\rho^\star = 500\rho_0$, the center of Ω is reached more or less quickly. With $\rho^\star = 1000\rho_0$, the peak of concentration does not reach the center, the progression is stopped after the last local peak has been "eaten". After this positioning, the concentration of bacteria "far" to the peak decreases continuously but very slowly. We have to take large time steps (physical time steps) in order to have significant variations of the variables and consequently of the density ρ in the numerical scheme and reach as quick as possible something like a "stationary solution".

In the following analysis reports, we add the percentage of area represented by the triangles retained for numerical integration (ie triangles where the density is $\geq \rho_{th}$, threshold value)

Quantitative results for $\rho^\star = 50\rho_0$

```
------------------------------------------------ Mesh 2
... Process time :   550.0 s  Total bacteria mass: 1.87500E+05    Threshold value: 1.00000E+06
---------------------------  Local max number: 1
*** J1 =  5379    Conc: 2.074E+08  (XG,YG)= ( 7.233E-01, 2.493E-01) (cmXcm)
    Number of triangles  N(1)=    277          Area % =   1.3118
    Local_Mass(1)  =  1.79917E+05 Percent(1)          =  95.95565 %
    Contrib(  5379)=  1.11379E+03 Percent_max_local(1)=   0.61906 %    Percent_max_total(1)=   0.59402 %
 -------- Global results ------
    Number of local maxima : 1    Total number of triangles  N=   277  Area % :  1.3118
    Troncated_Mass : 1.79917E+05  Troncated_Mass_Percent : 95.95565 %

------------------------------------------------ Mesh 2
... Process time :223220.0 s  Total bacteria mass: 1.87500E+05    Threshold value: 1.00000E+06
---------------------------  Local max number: 1
*** J1 =  5432    Conc: 2.670E+08  (XG,YG)= ( 7.484E-01, 2.486E-01) (cmXcm)
    Number of triangles  N(1)=    199          Area % =   1.0750
    Local_Mass(1)  =  1.87157E+05 Percent(1)          =  99.81688 %
    Contrib(  5432)=  1.40406E+03 Percent_max_local(1)=   0.75021 %    Percent_max_total(1)=   0.74883 %
 -------- Global results ------
    Number of local maxima : 1    Total number of triangles  N=   199  Area % :  1.0750
    Troncated_Mass : 1.87157E+05  Troncated_Mass_Percent : 99.81688 %
```

Quantitative results for $\rho^\star = 500\rho_0$

```
------------------------------------------------
... Process time :   100.0 s  Total bacteria mass: 1.87500E+05    Threshold value: 1.00000E+06
---------------------------  Local max number: 1
*** J1 =  2622    Conc: 5.173E+08  (XG,YG)= ( 2.930E-01, 2.493E-01) (cmXcm)
    Number of triangles  N(1)=   2441          Area % =  15.4336
    Local_Mass(1)  =  1.63828E+05 Percent(1)          =  87.37489 %
    Contrib(  2622)=  2.77833E+03 Percent_max_local(1)=   1.69589 %    Percent_max_total(1)=   1.48178 %
 -------- Global results ------
    Number of local maxima : 1    Total number of triangles  N=  2441  Area % : 15.4336
    Troncated_Mass : 1.63828E+05  Troncated_Mass_Percent : 87.37489 %
------------------------------------------------
```

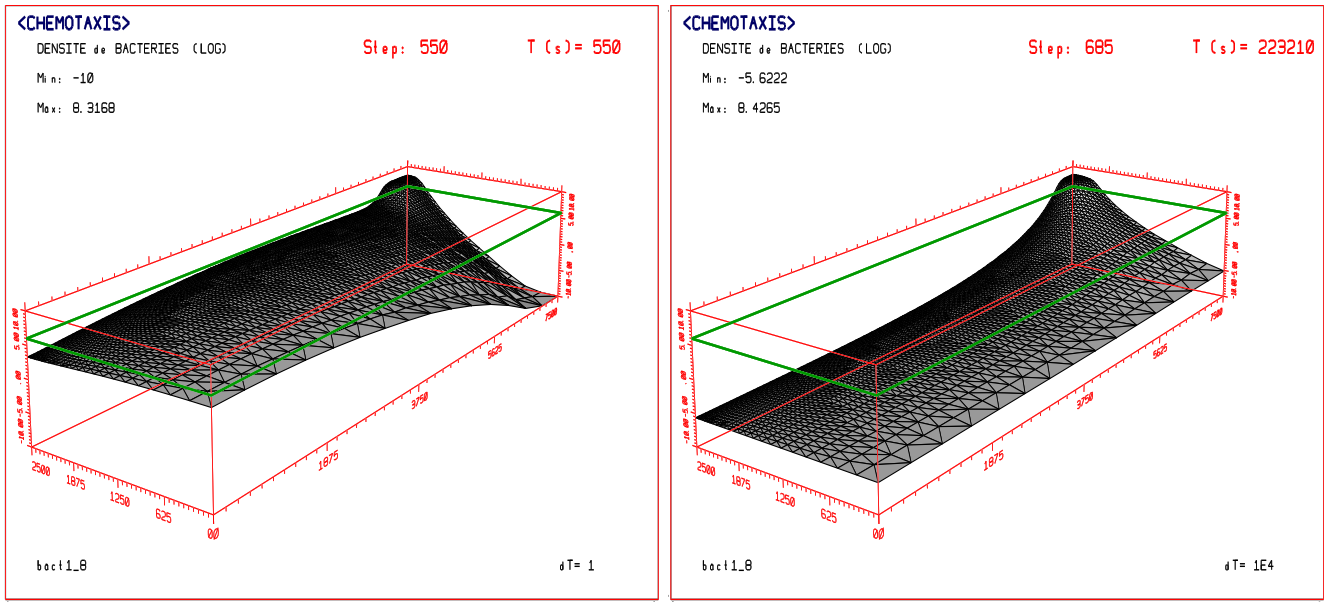

(a) High concentration localization after 550s (b) Distribution after large simulation time

Figure 10: Bacteria concentration, (Log. scale). *Computational domain:rectangle* $0.75cm \times 0.25cm$. *Bounded production of attractants* ($\rho^\star = 50\rho_0$), *observer position near* (x_{min}, y_{min}).

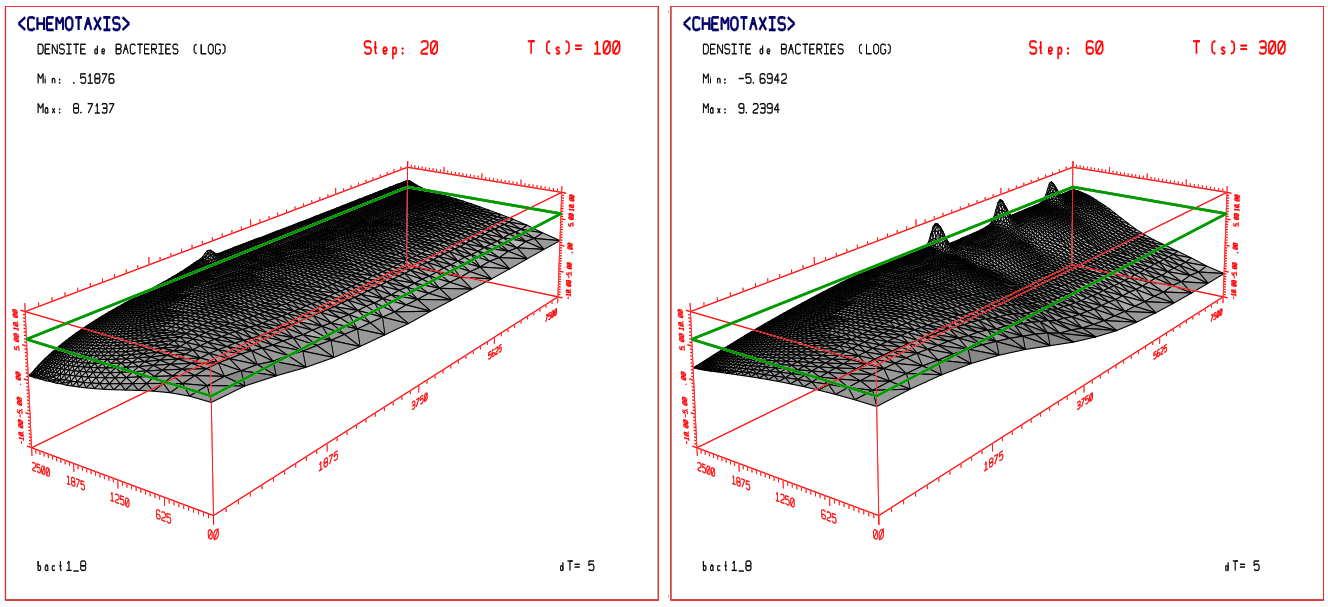

(a) High concentration localization after 100s (b) High concentration localization after 300s

Figure 11: Bacteria concentration, (Log. scale). *Computational domain:rectangle* $0.75cm \times 0.25cm$. *Bounded production of attractants* ($\rho^\star = 500\rho_0$), *observer position near* (x_{min}, y_{min}).

```
... Process time :   300.0 s  Total bacteria mass: 1.87500E+05    Threshold value: 1.00000E+06
----------------------------  Local max number: 1
*** J1 =  3358    Conc: 1.735E+09  (XG,YG)= ( 4.138E-01, 2.486E-01) (cmXcm)
```

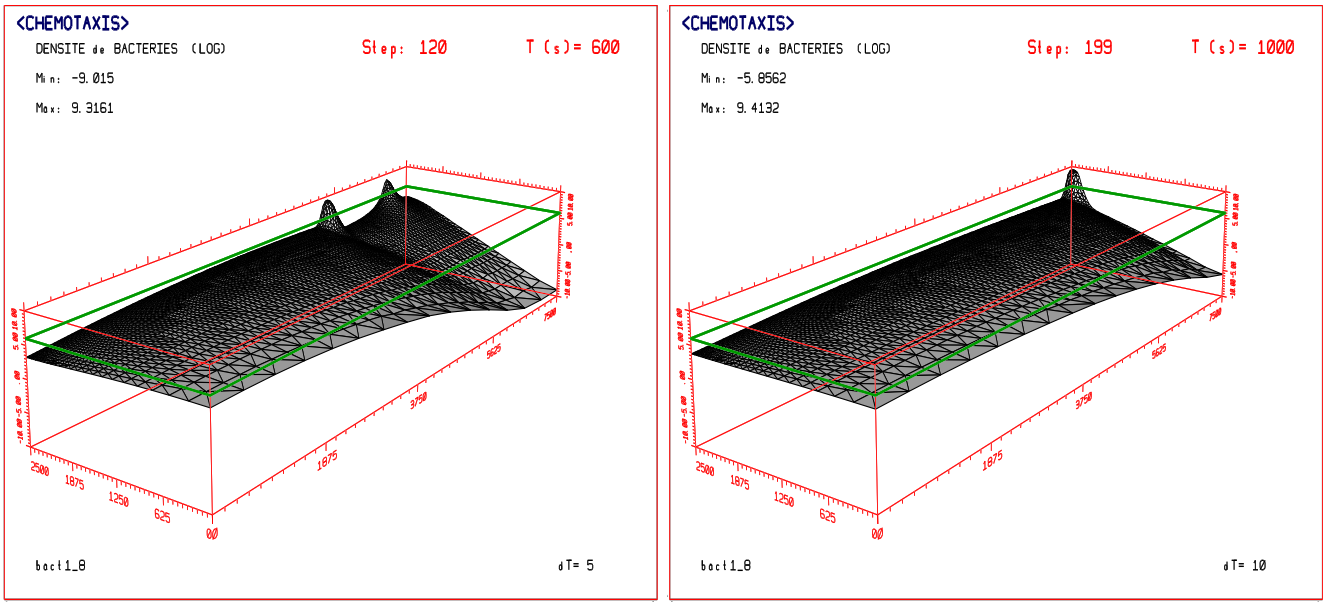

(a) High concentration localization after 600s (b) High concentration localization after 1000s

Figure 12: Bacteria concentration, (Log. scale). *Computational domain:rectangle* $0.75cm \times 0.25cm$. *Bounded production of attractants* ($\rho^\star = 500\rho_0$), *observer position near* (x_{min}, y_{min}).

```
    Number of triangles  N(1)=     57          Area % =   0.2050
    Local_Mass(1)   =  9.84080E+04 Percent(1)          =  52.48427 %
    Contrib(  3358)=  9.09209E+03 Percent_max_local(1)=   9.23918 %    Percent_max_total(1)=   4.84911 %
---------------------------  Local max number: 2
*** J2 =  4338    Conc: 1.342E+09  (XG,YG)= ( 5.601E-01, 2.486E-01) (cmXcm)
    Number of triangles  N(2)=     51          Area % =   0.1813
    Local_Mass(2)   =  5.36993E+04 Percent(2)          =  28.63965 %
    Contrib(  4338)=  7.56914E+03 Percent_max_local(2)=  14.09541 %    Percent_max_total(2)=   4.03688 %
---------------------------  Local max number: 3
*** J3 =  5207    Conc: 8.238E+08  (XG,YG)= ( 6.881E-01, 2.493E-01) (cmXcm)
    Number of triangles  N(3)=     55          Area % =   0.1963
    Local_Mass(3)   =  2.53662E+04 Percent(3)          =  13.52863 %
    Contrib(  5207)=  4.42463E+03 Percent_max_local(3)=  17.44302 %    Percent_max_total(3)=   2.35980 %
---------------------------  Local max number: 4
*** J4 =  2925    Conc: 1.193E+06  (XG,YG)= ( 3.433E-01, 2.493E-01) (cmXcm)
    Number of triangles  N(4)=    102          Area % =   0.3556
    Local_Mass(4)   =  7.28307E+02 Percent(4)          =   0.38843 %
    Contrib(  2925)=  6.40780E+00 Percent_max_local(4)=   0.87982 %    Percent_max_total(4)=   0.00342 %
 -------- Global results ------
    Number of local maxima : 4    Total number of triangles  N=   265  Area % :  0.9383
    Troncated_Mass : 1.78202E+05  Troncated_Mass_Percent : 95.04099 %
-----------------------------------------------
... Process time :   600.0 s  Total bacteria mass: 1.87499E+05    Threshold value: 1.00000E+06
---------------------------  Local max number: 1
*** J1 =  4240    Conc: 2.070E+09  (XG,YG)= ( 5.425E-01, 2.493E-01) (cmXcm)
    Number of triangles  N(1)=     63          Area % =   0.2316
    Local_Mass(1)   =  1.56721E+05 Percent(1)          =  83.58472 %
    Contrib(  4240)=  1.11202E+04 Percent_max_local(1)=   7.09557 %    Percent_max_total(1)=   5.93081 %
---------------------------  Local max number: 2
*** J2 =  5250    Conc: 8.198E+08  (XG,YG)= ( 6.963E-01, 2.486E-01) (cmXcm)
    Number of triangles  N(2)=     53          Area % =   0.1891
    Local_Mass(2)   =  2.57054E+04 Percent(2)          =  13.70959 %
    Contrib(  5250)=  4.29516E+03 Percent_max_local(2)=  16.70921 %    Percent_max_total(2)=   2.29076 %
 -------- Global results ------
    Number of local maxima : 2    Total number of triangles  N=   116  Area % :  0.4207
```

```
    Troncated_Mass : 1.82426E+05  Troncated_Mass_Percent : 97.29431 %
-----------------------------------------------
... Process time :  1000.0 s  Total bacteria mass: 1.87500E+05    Threshold value: 1.00000E+06
----------------------------  Local max number: 1
*** J1 =  5432    Conc: 2.589E+09  (XG,YG)= ( 7.484E-01, 2.486E-01) (cmXcm)
    Number of triangles  N(1)=     39          Area % =   0.1455
    Local_Mass(1)  =  1.83725E+05 Percent(1)          =  97.98692 %
    Contrib(  5432)=  1.36181E+04 Percent_max_local(1)=   7.41218 %    Percent_max_total(1)=   7.26297 %
 -------- Global results ------
    Number of local maxima : 1    Total number of triangles  N=    39  Area % :  0.1455
    Troncated_Mass : 1.83725E+05  Troncated_Mass_Percent : 97.98692 %
```

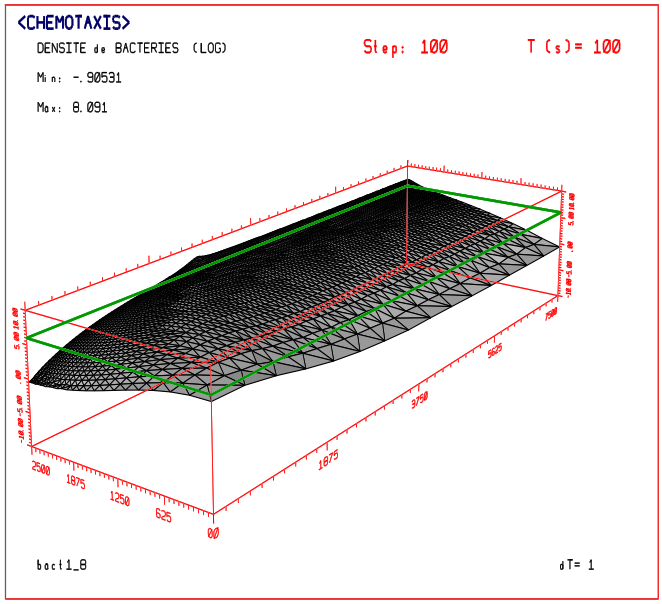

(a) High concentration localization after 100s

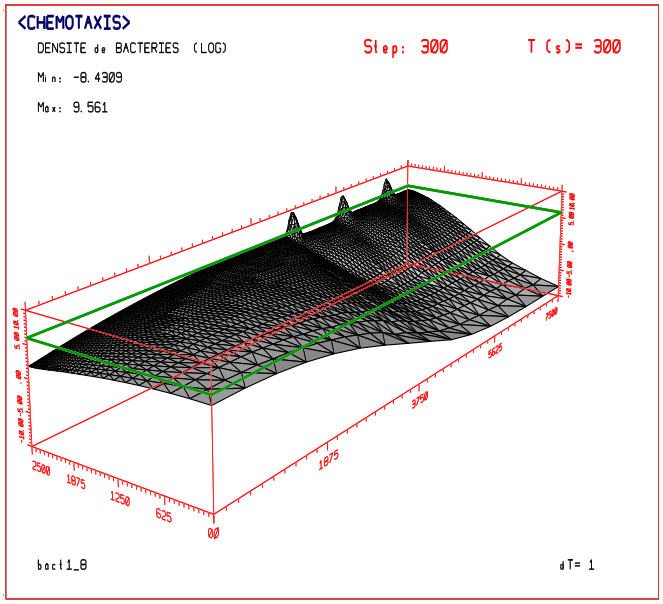

(b) High concentration localization after 300s

Figure 13: Bacteria concentration, (Log. scale). *Computational domain:rectangle* $0.75cm \times 0.25cm$. *Bounded production of attractants* ($\rho^\star = 1000\rho_0$), *observer position near* (x_{min}, y_{min}).

Quantitative results for $\rho^\star = 1000\rho_0$, *"Stationary solution"*.

```
-----------------------------------------------
... Process time :******** s  Total bacteria mass: 1.87534E+05    Threshold value: 1.00000E+06
----------------------------  Local max number: 1
*** J1 =  4953    Conc: 4.422E+09  (XG,YG)= ( 6.479E-01, 2.493E-01) (cmXcm)
    Number of triangles  N(1)=     38          Area % =   0.1325
    Local_Mass(1)  =  1.87473E+05 Percent(1)          =  99.96752 %
    Contrib(  4953)=  2.37528E+04 Percent_max_local(1)=  12.67000 %    Percent_max_total(1)=  12.66588 %
 -------- Global results ------
    Number of local maxima : 1    Total number of triangles  N=    38  Area % :  0.1325
    Troncated_Mass : 1.87473E+05  Troncated_Mass_Percent : 99.96752 %
```

Conclusion

We have presented here a computational scheme which allows the simulation of chemotactic bacteria aggregation. As theoretically predicted, the density redistribution during the evolution process

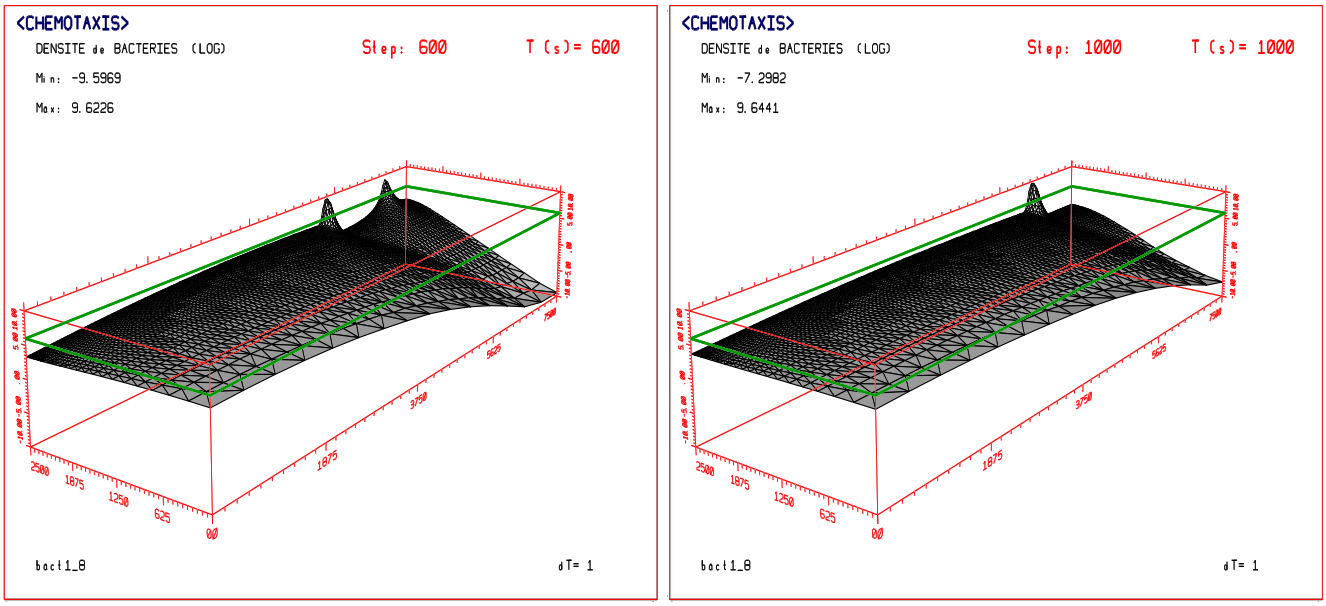

(a) High concentration localization after 600s (b) High concentration localization after 1000s

Figure 14: Bacteria concentration, (Log. scale). *Computational domain:rectangle* $0.75cm \times 0.25cm$. *Bounded production of attractants* ($\rho^\star = 1000\rho_0$), *observer position near* (x_{min}, y_{min}).

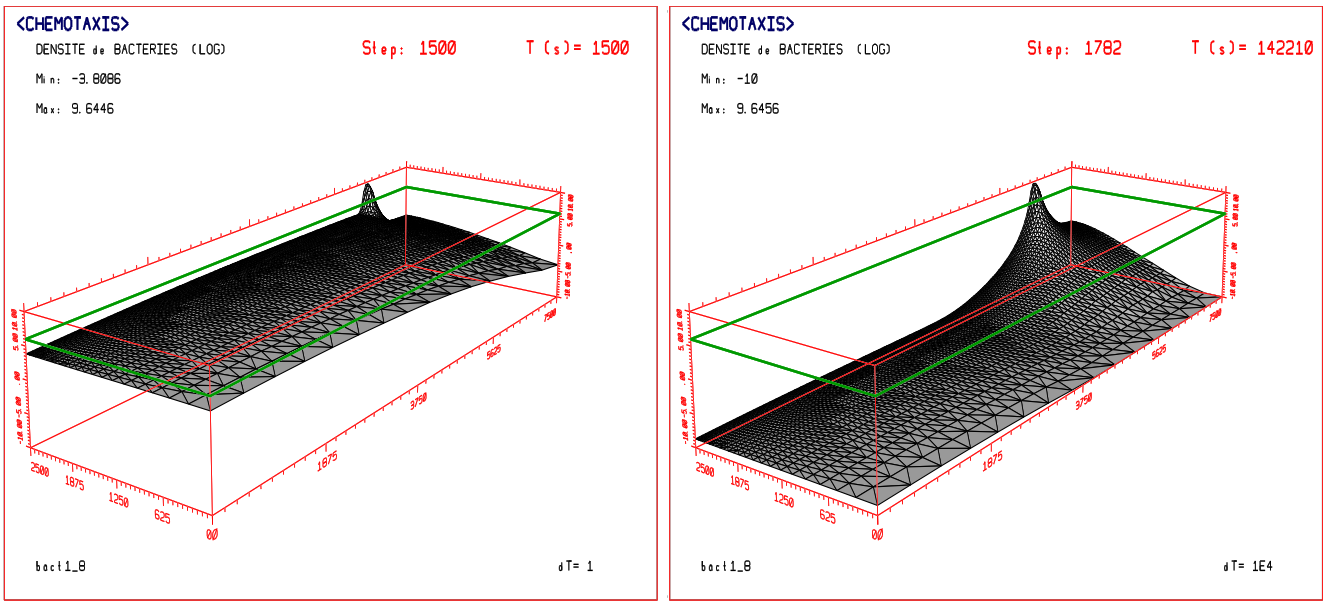

(a) High concentration localization after 1500s (b) Distribution after a long time

Figure 15: Bacteria concentration, (Log. scale). *Computational domain:rectangle* $0.75cm \times 0.25cm$. *Bounded production of attractants* ($\rho^\star = 1000\rho_0$), *observer position near* (x_{min}, y_{min}).

appears to be strongly dependent on the model used for the source (production) of attractants. With the first model (source of attractants proportional to the bacterial density ρ), several isolated

peaks of bacterial concentration may appear -concentration localized over only one element, which is something like a Dirac mass at discrete level- and remain more or less at the same place along the evolution process.

Introducing a cutoff value in the production of attractants, the first peak of bacterial concentration travels to the center of the domain, "eliminating" all the secondary peaks. After a certain amount of time, high densities values remain localized on small part of the domain (0.1 to 1 %) but not only over one mesh element.

Acknowledgments

Many thanks to B. Perthame for fruitful discussions and for relevant suggestions concerning this work.

References

[1] E.F. Keller and L.A. Segel. Model for chemotaxis. *J. Theor. Biol.*, 30:225–234, 1971.

[2] M. D. Betterton and M. P. Brenner. Collapsing bacterial cylinders. *Phys. Rev. E*, 64(061904), 2001.

[3] M.P. Brenner, P. Constantin, L.P. Kadanoff, A. Schenkel, and S.C. Venhataramani. Diffusion, attraction and collapse. *Nonlinearity*, 12(4):1071–1098, 1999.

[4] M.P. Brenner, L.S. Levitov, and E.O. Budrene. Physical mechanisms for chemotactic pattern formation bybacteria. *Biophysical Journal*, 74:1677–1693, 1998.

[5] L. Corrias, B. Perthame, and H. Zaag. A model motivated by angiogenesis. *C. Rendus Acad. Sc. Paris*, to appear.

[6] W. Jäger and S. Luckhaus. On explosion of solution to a system of partial differential equations modelling chemotaxis. *Trans. Amer. Math. Soc.*, 239(2):819–824, 1992.

[7] M.A. Herrero, E. Medina, and J.J.L. Velázquez. Finite time aggregation into a single point in a reaction-diffusion system. *Nonlinearity*, 10(6):1739–1754, 1997.

[8] M.A. Herrero and J.J.L. Velázquez. Chemotactic collapse for the keller-segel model. *J. Math. Biol.*, 35(2):177–194, 1996.

[9] F. Hecht and A. Marrocco. Numerical simulation of heterojunction structures using mixed finite elements and operator splitting. In R. Glowinski, editor, *10th International Conference on Computing Methods in Applied Sciences and Engineering*, pages 271–286, Le Vésinet, February 1992. Nova Science Publishers,Inc.

[10] F. Hecht and A. Marrocco. Mixed finite element simulation of heterojunction structures including a boundary layer model for the quasi-fermi levels. *COMPEL*, 13(4):757–770, december 1994.

[11] A El Boukili and A. Marrocco. Arclength continuation methods and applications to 2d drift-diffusion semiconductor equations. Rapport de recherche 2546, INRIA, mai 1995.

[12] A. El Boukili. *Analyse mathématique et simulation numérique bidimensionnelle des dispositifs semiconducteurs à hétérojonctions par l'approche éléments finis mixtes.* PhD thesis, Univ. Pierre et Marie Curie, Paris, décembre 1995.

[13] A. Marrocco and Ph. Montarnal. Simulation des modèles energy-transport à l'aide des éléments finis mixtes. *C.R. Acad. Sci. Paris*, 323(Série I):535–541, 1996.

[14] Ph. Montarnal. *Modèles de transport d'énergie des semi-conducteurs, études asymptotiques et résolution par des éléments finis mixtes.* PhD thesis, Université Paris VI, octobre 1997.

[15] R. Glowinski and P. Le Tallec. *Augmented Lagrangian and Operator Splitting Methods in Nonlinear Mechanics.* Studies in Applied Mathematics. SIAM, Philadelphia, 1989.

Unité de recherche INRIA Rocquencourt
Domaine de Voluceau - Rocquencourt - BP 105 - 78153 Le Chesnay Cedex (France)

Unité de recherche INRIA Lorraine : LORIA, Technopôle de Nancy-Brabois - Campus scientifique
615, rue du Jardin Botanique - BP 101 - 54602 Villers-lès-Nancy Cedex (France)
Unité de recherche INRIA Rennes : IRISA, Campus universitaire de Beaulieu - 35042 Rennes Cedex (France)
Unité de recherche INRIA Rhône-Alpes : 655, avenue de l'Europe - 38330 Montbonnot-St-Martin (France)
Unité de recherche INRIA Sophia Antipolis : 2004, route des Lucioles - BP 93 - 06902 Sophia Antipolis Cedex (France)

Éditeur
INRIA - Domaine de Voluceau - Rocquencourt, BP 105 - 78153 Le Chesnay Cedex (France)
http://www.inria.fr
ISSN 0249-6399